Efficient Speed Advisories for Multi-Stage-Metering Arrival Management

Jesper Bronsvoort, Greg McDonald, & Meru Soni
ATM Automation - Airservices Australia
GPO Box 1093, Tullamarine VIC 3043, Australia
jesper.bronsvoort|greg.mcdonald|meru.soni@airservicesaustralia.com

Juan Alberto Besada
Data Processing and Simulation Group – Universidad Politécnica de Madrid
Despacho C-321 ETSI Telecomunicación, 28040 Madrid, Spain
besada@grpss.ssr.upm.es

***Abstract* – This paper presents a methodology and algorithm for Air Traffic Control (ATC) to efficiently achieve schedules arrival times through speed control in the presence of uncertainty. The methodology does not assume the availability of airborne time of arrival control and can therefore be applied to legacy aircraft. The speed advisories are calculated in a manner that allows for sufficient control margin to, if required, adjust the aircraft's trajectory at a later stage to correct for estimated arrival time drift at the lowest impact to efficiency. The methodology is therefore envisioned to prevent major last-minute interventions and instead assists ATC in allowing more continuous descent approaches to be conducted by aircraft leading to more efficient operations.**

Index Terms: *Air Traffic Management; Air Traffic Control; Operational Concept; Arrival Management*

I. Introduction

Much attention is given around the world to develop a concept of operations that improves on current arrival management by allowing onboard automation to conduct a descent along an efficient profile that better reflects the user intentions and preferences. Due to limited predictive support to ATC, sequencing actions are performed close to the destination, thus impacting on such a preferred descent profile. An improvement to this situation would be if sequencing actions were performed earlier, when the aircraft is still cruising, allowing the flight crew to efficiently adopt any constraints into the planned descent trajectory.

With this objective, both SESAR and NextGen propose that aircraft will be assigned a time at a metering point which they must achieve within a tight tolerance [1; 2]. Modern Flight Management Systems (FMSs) can adopt such an assigned time while optimising the descent profile and provide closed-loop control to meet the time constraint (Required Time of Arrival (RTA) functionality). In order to do this, the control variable in the aircraft's operation used to attain the assigned time, is speed. Any unexpected speed change by an aircraft will cause increased workload to a controller as the impact of such a change is assessed [3; 4]. In addition it will take significant time before, and if, all aircraft will be equipped with this functionality.

At the 2012 ATOS conference in Delft, The Netherlands, we presented an operational concept for arrival management using multiple metering points strategically chosen along an aircraft's trajectory [5]. The concept envisions aircraft conducting a continuous descent based on a consistent speed schedule instructed by ATC and relies on current FMS descent guidance strategies available on most modern commercial aircraft. ATC is subsequently supported by accurate ground-based trajectory prediction to manage the temporal uncertainty though metering at the strategically chosen points along the intended trajectory of the aircraft.

This paper supports the above concept with a detailed discussion of the sequence resolutions chosen to effect the multi-stage metering. In particular it will discuss how a ground-based Decision Support Tool relying on accurate trajectory prediction could generate speed advisories to deliver individual aircraft at the metering points within allowed tolerances.

II. Background

To enable a continuous descent to occur for an aircraft, it must be sequenced and facilitated with all other operations. To enable the aircraft automation to operate to the threshold without route discontinuities and manual pilot intervention, a structured terminal area (TMA) with runway-linked Standard Terminal Arrival Routes (STARs) is desirable. A defined lateral path to the threshold enables the FMS to compute a continuous descent profile within a set of given constraints (e.g. speed and altitude constraints). Therefore to allow the FMS to plan and conduct a continuous descent, the aircraft it must be sequenced well prior to Top of Descent (TOD) and thus enabling its descent to be continuous but at a time desired by ATC.

Erzberger et al. of NASA were one the first to propose an automated concept to traffic management in the TMA in the 1980's [6; 7]. A scheduler generates the landing sequence and associated conflict-free landing times. The concept envisions that conflict-free landing times will be uplinked to sufficiently equipped aircraft for which the onboard automation determines the appropriate control commands (e.g. RTA). For the unequipped aircraft a ground-based system determines the appropriate commands to meet the conflict-free arrival time, which are subsequently communicated via voice to the pilot. Based on

this principle the Efficient Descent Advisor (EDA) was developed by NASA [8]. EDA has been used to assist the Tailored Arrivals program in San Francisco (SFO) where a route clearance to the runway threshold, complete with altitude crossing constraints, was uplinked to qualifying aircraft [9]. These aircraft were subsequently allowed to perform an idle-thrust descent while meeting these constraints. EDA determined the speed schedule (cruise Mach and descent Calibrated Airspeed (CAS)) in order to meet the arrival time as set by the arrival manager.

Based on the principle of EDA, the Speed And Route Advisory (SARA) function has been developed for Amsterdam Schiphol Airport. The objective of the SARA function is to deliver advisories on speed and/or routing in order to achieve a predetermined time at the Initial Approach Fix (IAF) [10]. At first only speed advice is attempted in order to achieve the required IAF time. If speed only does not suffice additional track miles are added. Operational trials demonstrated benefits, however because of Amsterdam's complex airspace structure, speed advisories could often only be given after the aircraft had commenced descent [11]. Any speed advisories given are then too late for the FMS to appropriately adopt into the descent profile.

Speed advisories given around or just after TOD only provide limited sequence resolution to a TMA entry point. Often much larger delays need to be absorbed by aircraft to fit in their landing slot, thus calling for coarse sequencing to be performed prior to TOD.

III. Multi Stage Metering

In Australia a concept is being researched in which in aircraft are being sequenced to their runway slot time though metering at multiple strategically chosen points along the aircraft's trajectory [5]. In addition to the traditional Metering Fix at Terminal Area (TMA) entry, a new sequencing point in the final phase of cruise called the Outer Fix is introduced. The outer sector controller will achieve the scheduled Outer Fix time through (cruise) speed change and if necessary path stretching. At or prior to reaching the Outer Fix the aircraft will be advised with a revised descent speed schedule to achieve the scheduled Metering Fix time. Beyond the Metering Fix precise sequencing in the form of radar vectoring will be applied if necessary to fine-tune the sequence at the runway threshold and maintain runway capacity.

The process will be further illustrated by means of an example. In Fig. 1 an aircraft is at a point prior to descent and from its current position, path and speed a Trajectory Predictor (TP) calculates an Estimated Time of Arrival (ETA) for the Outer Fix, Metering Fix and the runway threshold. Effectively, the dashed line provides a reference to the ETA at a particular position ahead of the aircraft continuous with distance. These estimates contain some uncertainty as the models for aircraft intent, aircraft performance model and forecast weather are not perfect. The uncertainty can be statistically quantified through historical performance of the respective TP [12]. The shaded area provides an indication of the uncertainty, quantified as the historical 95% containment area, as it grows with prediction horizon (distance away from current position). These models are similar to those developed by EUROCAE Working Group 85 (WG85) for ETA uncertainty in both open loop and closed loop (RTA) operations based on the sources of this uncertainty [13; 14].

Suppose the aircraft in Fig 1 is assigned with a scheduled time of arrival (STA) at the runway threshold by the arrival manager. From this STA, subsequently STAs for the Metering Fix and Outer Fix can be derived based on a nominal speed schedule. Similar to the line indicating the ETA continuous with distance, a line can be added to indicate the STA continuous with distance; this continuous STA coincides at the Outer Fix and Metering Fix with the respective discrete STA values. Therefore in Fig. 1, the STA lines provide an indication of where the aircraft should be in order to be 'on schedule'. In the example the ETA line is above the STA line and hence currently the aircraft is late. Previously the different tolerances for the Outer Fix, Metering Fix and runway threshold were presented and are these are also indicated in Fig 1.

In the proposed concept, a speed schedule amendment, and if necessary a route amendment, are issued to affect the delay into the outer fix (Fig. 2). With speed (and route) advisory, the aircraft's ETA line now coincides with the RTA line. However because it is so far out – prior to descent – the prediction uncertainty delta of the estimate at the runway and Metering Fix is larger than the target time window. However in terms of the Outer Fix the uncertainty is entirely contained within the tolerance because of the first sequence instruction. Therefore the aircraft is permitted to proceed without further intervention to at least the Outer Fix, and with the expectation of a continuous descent thereafter. But as the uncertainty at the Metering Fix is larger than the tolerance, the descent speed for that continuous descent might have to be adjusted. The situation would need to be monitored by the controller assisted by ATC automation until the aircraft comes close enough to a target window (e.g. Metering Fix) such that the uncertainty for its respective estimate is entirely contained within the tolerance. Practically what it means is that if the uncertainty is not fully contained within the target window, there is a probability larger than 5% that any sequence instruction derived by the TP is not effective (refer to WG85 ETA

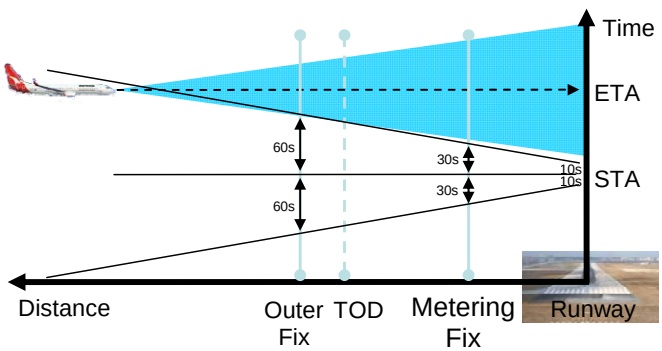

Figure 1: Aircraft assigned with STA.

uncertainty modelling activities [13; 14]).

Now consider Fig. 3, the aircraft has progressed and the ETA has drifted away from the STA as there is no closed-loop control in the time dimension. Still the aircraft will achieve the target window at the Outer Fix within acceptable buffer but not the Metering Fix. Therefore an adjustment in speed schedule will be derived by the TP and delivered to the aircraft to shift the ETA at the Metering Fix to the STA (Fig. 4). The applied speed should be maintained until mandated speed changes e.g. 250 knots CAS (KCAS) below ten thousand feet. This intervention issued before TOD will enable an efficient and continuous descent at a speed that puts the aircraft back into the defined sequence position and the aircraft is allowed to conduct an efficient continuous descent. Lateral path amendments after TOD should be avoided to maintain the integrity of a structured TMA.

The aircraft in Fig. 5 will achieve the Metering Fix within the target window but will be outside the target window for the threshold (early). Consequently the aircraft will require TMA speed adjustment or minor radar vectoring to achieve the time at the runway. This radar vectoring, if required, is envisioned to be a small adjustment within the circuit area and should occur before the start of an instrument approach or RNP arrival procedure.

Note that while multiple sequence actions might occur, the STA for the aircraft has not changed, like the STA for all the other aircraft in the sequence have not changed; ATC is operating to a consistent plan as set by the arrival manager, which can operate to a larger sequence horizon.

In summary, sequence resolution will be a three phase approach (if necessary):

1. Coarse sequencing or the largest delay occurring before the Outer Fix and descent commencing. Note there is scope to enhance by rough sequencing by ground delay programmes.
2. Fine sequencing by assigning a specific descent speed so the aircraft automation adjusts its descent point and path to cross the Metering Fix at the desired time.
3. Precise sequencing using radar vectoring similar to techniques of today but expected to be used far less often due to the tighter sequencing to the Metering Fix.

For this multi-stage long distance sequencing, it is anticipated that ATC will be assisted in providing effective sequence resolution actions by appropriate automation in the form of Decision Support Tools (DSTs) like EDA and SARA. This paper will present the logic required for such automation systems in generating efficient and effective sequence resolutions.

IV. Efficient Absorption of Delay

To resolve delay, ATC can change an aircraft's trajectory in several ways. From an efficiency perspective the preferred order in which to absorb delay is through first speed reduction, then flight level changes, and finally path stretches and holding [15; 16]. The main focus in this paper will be on the use of speed reduction to achieve a delay.

Speed reduction consists of two degrees of freedom: cruise Mach number and descent CAS. To reduce dimensionality, it is convenient to assume a particular relationship between cruise Mach and descent CAS. For

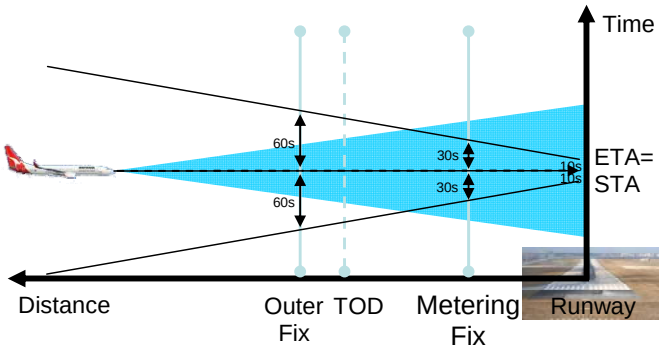

Figure 2: Sequence instruction into Outer Fix affected.

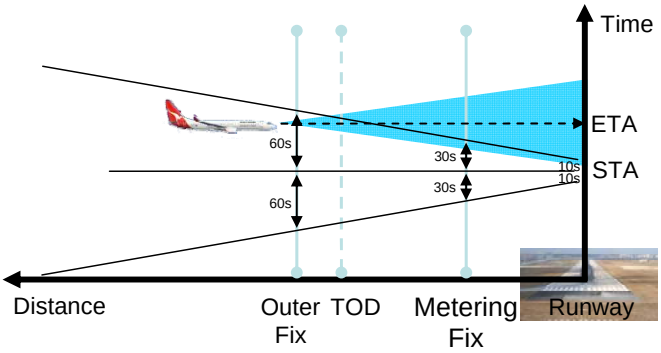

Figure 3: Aircraft late, but within time window at Outer Fix but not at Metering Fix.

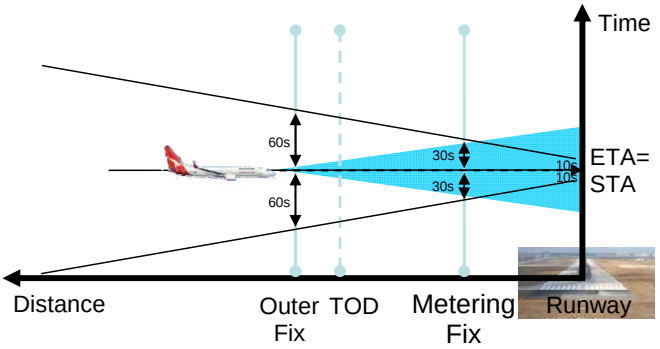

Figure 4: Sequence instruction into Metering Fix affected.

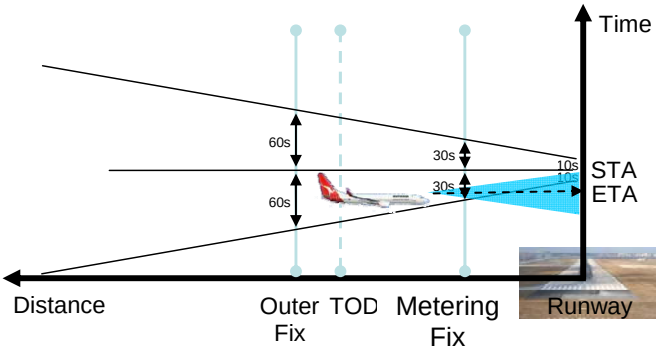

Figure 5: Aircraft in tolerance but threshold ETA early.

example, EDA assumes a proportional linear relationship between cruise Mach and descent CAS changes to reduce iteration to a single parameter [7]. While this linear relationship provides a single, convenient, and computationally fast rule of thumb, the relationship between cruise Mach and descent CAS leading to minimum fuel burn for a given flight time is however non-linear [16]. Thus by assuming a linear relationship, non-optimal speed schedules can result. Modern FMS use Cost Index (CI) alteration to find the appropriate combination of cruise Mach and descent CAS to meet a time constraint [17]. Changing the CI changes the relationship between fuel costs and time costs resulting in different target speeds to be derived [15]. Effectively, the CI takes the role of the parameter coupling cruise Mach and descent CAS in a non-linear relationship.

The relationship of CI between cruise Mach and descent CAS within the FMS is proprietary and therefore not publically available. In the next sections simulations will be performed to empirically derive a robust non-linear relationship that approximates the optimal coupling between cruise Mach and descent CAS.

V. Problem Statement

This paper presents a generic methodology that can be applied to provide efficient speed advisories. These speed advisories will be issued when the aircraft is still on cruise and therefore contain sufficient control margin to allow for adjustments required at a later stage. Objective is to find the relationships that couple the various degrees of freedom available to provide sequence resolutions into a single variable, the cruise Mach number, while respecting these objectives and constraints. The found relationships can subsequently be used by a Decision Support Tool to generate sequence resolution advisories to meet a certain STA while iterating in a single variable, as represented by the sequence resolution logic in Fig. 6.

VI. Simulation Scenario

The scenario studied for the simulations is an aircraft appearing at a sequence horizon of 250NM from the destination cruising at FL380. For a range of cruise mach numbers and descent CAS, the flight time and fuel burn for these final 250NM are determined. The following intent is assumed based on generic operations:

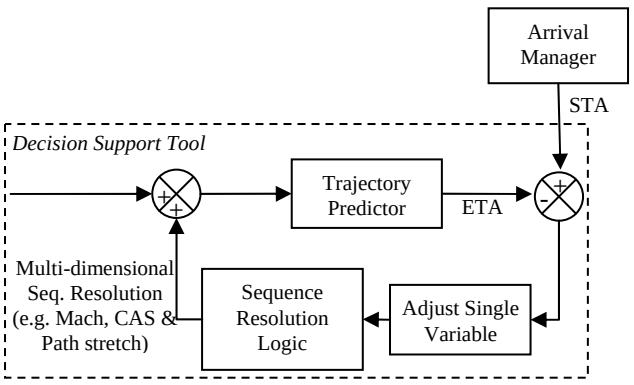

Figure 6: Sequence Resolution Process Model.

- Cruise Mach number is propagated into the descent and held until crossover occurs to the descent CAS. If the descent CAS is lower than the CAS resulting from the cruise Mach number at cruising altitude, a slope deceleration is modelled at -1000ft/min.
- A generic TMA 250KCAS speed constraint is modelled at 10,000ft. The deceleration from the descent CAS to 250KCAS is modelled by a slope deceleration at -500ft/min (if deceleration is required). If a combination of Mach and CAS results in cross-over below 10,000ft, the combination is ignored as operationally impracticable.
- A 180KCAS speed constraint is modelled at 3,000ft affected by a -500ft/min slope deceleration accompanied by appropriate flap selection.
- From 3,000ft a -3 degree slope is modelled to the runway threshold along which the aircraft is allowed to decelerate to 140KCAS accompanied by appropriate flap selection.

The aircraft assumed in the simulations is a Boeing 737-800 (B738) with initial mass of 63,000kgs. The aircraft performance calculations are based on models provided by Boeing Research & Technology Europe (BR&TE), which are of similar nature to the EURCONTROL Base of Aircraft Data (BADA) 4 models. Finally, International Standard Atmosphere (ISA) conditions are assumed.

The solution space of allowed airspeeds is bounded by:

$$\begin{aligned} 230\text{KCAS} \le V_{\text{CAS}} \le V_{MO} - 10\text{kts}, \\ M_{buffet} + 0.03 \le M \le M_{MO} - 0.015, \end{aligned} \quad (1)$$

where V_{MO} is the maximum operating CAS, M_{buffet} the buffet limit and M_{MO} the maximum operation Mach. The lower limit of 230KCAS was chosen in accordance with the range speeds currently instructed by ATC. The margin on the buffet limit is purposely larger as of the uncertainty related to this figure (derived from aircraft performance model and mass dependent).

The trajectories were simulated with use of an experimental trajectory predictor ATP developed by Airservices Australia. ATP is a high fidelity trajectory predictor based on the Aircraft Intent Description Language (AIDL) developed by BR&TE [18] .

VII. Results

Fig. 7 provides the solution space for a fixed flight distance of 250NM and the intent described in the previous section for the airspeeds bounded by (1). The lower left corner does not contain any data as these combinations of Mach and CAS would result in a cross-over altitude below 10,000ft. The colour provides an indication of the fuel burn (in kilograms), and the contour lines of the flight time (in minutes). The red line connects the Mach and CAS combinations that resulted in the lowest fuel burn for a given flight time. It is quite evident this optimal relationship is non-linear. Assuming a nominal speed schedule of M.78/280KCAS one can see that to resolve delay, the

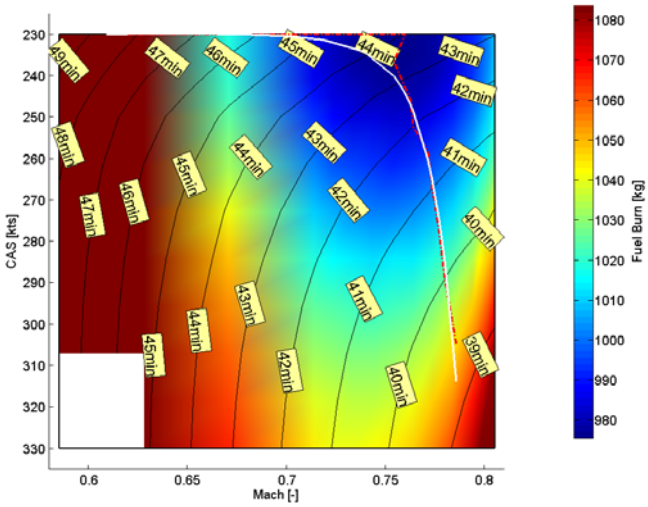

Figure 7: Solution space for B738/250NM/FL350.

optimal solution is initially much more sensitive to descent CAS changes than to cruise Mach changes. This is believed to be consistent with current RTA algorithms in the FMS where the descent speed is more sensitive to Cost Index alteration than the cruise Mach number (when within close range of destination).

The shape of the optimal solution line suggests an exponential fit can be made to couple Mach and CAS. To model the initial constant segment without the need of piece-wise fitting, the choice was made for a second order exponential fit of the following form

$$V_{\mathrm{CAS_{OPT}}} = V_{\mathrm{CAS}offset} + c_1 e^{c_2\left(M - M_{offset}\right) + c_3\left(M - M_{offset}\right)^2}. \quad (2)$$

The values for $V_{\mathrm{CAS}offset}$ and M_{offset} are chosen such that the second term in (2) nearly passes the origin for the valid Mach range. Therefore, in general

$$\begin{aligned} V_{\mathrm{CAS}offset} &= 230 - 0.5\,\mathrm{KCAS}, \\ M_{offset} &= M_{buffet} + 0.03. \end{aligned} \quad (3)$$

A linear least squares fit can easily be obtained by transforming (2) to

TABLE I
COEFFICIENTS FOR OPTIMAL MACH/CAS RELATIONSHIP (B738)

Altitude	Coefficients				
	c_1 [kts]	c_2 [-]	c_3 [-]	$V_{\mathrm{CAS}offset}$ [kts]	M_{offset} [-]
FL270	4.50E-01	4.48E+00	4.20E+01	229.5	0.466
FL280	4.44E-01	6.17E-01	5.87E+01	229.5	0.480
FL290	4.58E-01	4.02E+00	5.03E+01	229.5	0.494
FL300	4.34E-01	1.37E+00	6.64E+01	229.5	0.510
FL310	4.75E-01	-2.63E+00	8.34E+01	229.5	0.518
FL320	5.77E-01	-1.11E+01	1.26E+02	229.5	0.536
FL330	6.04E-01	-1.08E+01	1.41E+02	229.5	0.556
FL340	7.08E-01	-2.24E+01	2.05E+02	229.5	0.567
FL350	6.85E-01	-2.37E+01	2.45E+02	229.5	0.590
FL360	7.40E-01	-3.04E+01	3.10E+02	229.5	0.603
FL370	6.05E-01	-2.32E+01	3.47E+02	229.5	0.628
FL380	5.26E-01	-1.65E+01	3.58E+02	229.5	0.641
FL390	3.82E-01	6.53E+00	3.74E+02	229.5	0.672
FL400	3.54E-01	3.08E+01	2.90E+02	229.5	0.689
FL410	2.53E-01	8.62E+01	-9.65E+01	229.5	0.709

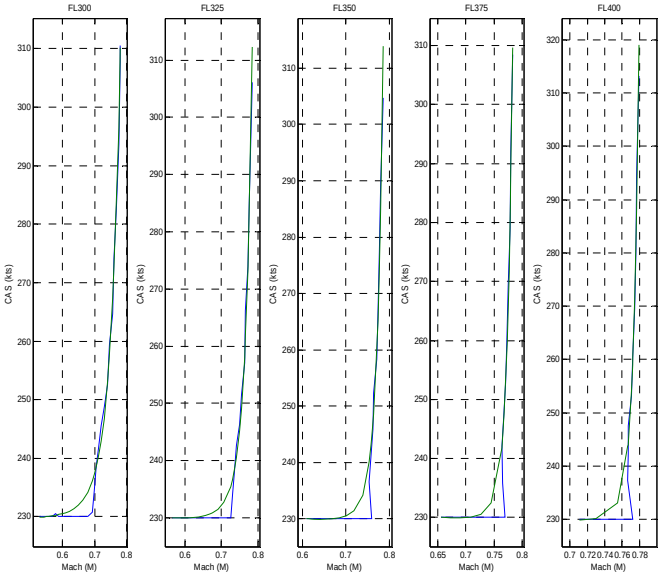

Figure 8: Solution space for B738/250NM/FL300-FL325-FL350-FL375-FL400 (blue: simulation minima; green: fit).

$$\ln\left(V_{\mathrm{CAS}} - V_{\mathrm{CAS}offset}\right) = \ln c_1 + c_2\left(M - M_{offset}\right) + c_3\left(M - M_{offset}\right)^2. \quad (4)$$

It is because of the logarithm in (4), that (2) cannot exactly pass the origin of the valid speed range.

It is important to note the region of lowest fuel burn Fb possible is a very flat (low dFb/dV_{CAS} and dFb/dM). Since the change in fuel burn over this region is very small (in the order of a few kg), any errors in the fit in that region will not cause any significant impact to fuel burn. Therefore a smaller weighting is applied in this region to make the fit better match the data in areas with higher fuel burn derivatives.

To observe how the general trend for the minimum fuel burn line varies with altitude, the model was run again from an altitude of 30,000ft to 40,000ft, in intervals of 2,500ft. Shown below in Fig. 8 is the resultant plot of this minimum fuel burn line for these initial altitudes. For each of the altitudes a fit was made as indicated by the green line. Again note the large difference between the fit (green) and the simulation minima (blue) in the lowest fuel burn region, but again the impact on fuel burn is not significant as of the low derivatives of fuel burn with airspeed.

An attempt was made to find a fit for the coefficients in (2) with altitude to define the entire problem analytically. This proved not to be successful due to the high sensitivity of (2), being second order exponential, to changes in the coefficients. Instead, the model was run for the range of initial altitudes FL270-FL410. As example, the coefficients for the B738 are presented in Table I.

Equation (2) supported by the coefficients in Table I provides the wanted relationship between cruise Mach and descent CAS for optimal delay absorption through speed control only.

The coefficients of Table I were derived for still wind conditions. To test this relationship for robustness against wind profiles, the simulation were once again run for both a

headwind and tailwind scenario. In both cases a linear changing wind with altitude was assumed with zero wind on the ground and 100kts wind at FL410. Fig. 13 till Fig. 21 (in the appendix) show the solution spaces for FL300, FL350 and FL400 for headwind, no wind and tailwind cases. The optimal relationship (2) has also been added for comparison against the simulation minima. As expected, the addition of wind has a significant impact on the range of flight times. But, as can be observed, the relation of optimal Mach and CAS coupling is not that sensitive to wind. The relationship (2) provides an adequate approximation of the simulation minima as differences in fuel burn are not significant. This is a fortunate finding as it appears that (2) with the coefficients from Table I can be applied irrespective of the wind conditions without significant impact.

VIII. Integration with Proposed Concept

As demonstrated by the results of the previous section, mostly the descent speed is changed to absorb delay optimally, meaning most of the delay absorption will occur during the final phases of flight leaving cruise speed fairly unchanged. If cruise conditions prove to be different to forecast such that the original delay needs to be adjusted, there might be little freedom left to change descent speed to achieve the adjusted delay in an efficient manner without reverting to conventional sequencing techniques such as open loop vectoring. Secondly, the use of speed control only might not be optimal as at some threshold point it becomes more efficient to perform path stretching than slowing the aircraft further down. In this section these two aspects will be addressed in terms of the proposed concept.

As discussed earlier in this paper, the proposed multi stage metering concept envisions that coarse sequencing is affected in the final cruise phase of flight. Suppose the horizon for this coarse sequencing is 250NM. If for the moment it is assumed that speed schedule alteration provides enough freedom to resolve delay, an approximate optimal solution can be found from the relationship derived in the previous section. If this solution is provided to the aircraft at 250NM out, and given this solution is in the form of a speed constraint (open-loop) rather than a time constraint (closed-loop), the estimated time of arrival can still drift while the aircraft is progressing to its destination as previously discussed and illustrated by Fig. 4. The concept allows a maximum deviation of 60 seconds from the STA over the Outer Fix. This deviation should subsequently be corrected by an amendment in the speed schedule to affect the sequence into the Metering Fix. Practically this means that when the first speed instruction is derived at 250NM out, a sufficient 'control margin' should be respected to allow for a maximum 60 seconds adjustment by speed schedule amendment at the Outer Fix. Effectively this control margin reduces the solution space previously introduced.

TABLE II
Coefficients for Control Boundaries at Outer Fix (B738)

		High speed boundary (+60 s)	Low speed boundary (-60 s)
d_0	[kts]	6.58E+03	1.52E+03
d_1	[kts/ft]	3.68E-01	-3.06E-02
d_2	[-]	-5.46E+00	1.13E-01
d_3	[kts]	-3.91E+04	-4.51E+03
d_4	[kts/ft^2]	1.18E-06	2.01E-06
d_5	[kts^{-1}]	9.99E-05	-1.98E-05
d_6	[kts]	7.05E+04	8.79E+03
d_7	[ft^{-1}]	-1.43E-04	-4.15E-05
d_8	[ft^{-1}]	-1.02E+00	-9.23E-02
d_9	[-]	1.98E+01	2.17E+00
d_{10}	[kts/ft^3]	0	0
d_{11}	[kts^{-2}]	0	0
d_{12}	[kts]	-3.95E+04	-8.25E+03
d_{13}	[ft^{-1}]	1.83E-04	5.02E-05
d_{14}	[ft^{-1} kts^{-1}]	0	0
d_{15}	[kts/ft]	7.04E-01	2.34E-01
d_{16}	[ft^{-1}]	0	0
d_{17}	[kts/ft^2]	-1.52E-06	-3.23E-06
d_{18}	[-]	-1.64E+01	-2.77E+00
d_{19}	[kts^{-1}]	0	0

The control boundaries can be determined by establishing the solution space at the Outer Fix horizon. Knowing the maximum and minimum flight time from the Outer Fix to the threshold (assuming nominal TMA transition), the Mach and CAS combinations can be determined that result in 60 seconds less than maximum, or 60 seconds more than minimum flight time. Such combinations were determined for the same range of initial cruising altitude (FL270-FL410), null wind, and the linear headwind/tailwind introduced earlier.

It must be noted that the dependency of the control boundary relationships on wind is much stronger than the optimal Mach/CAS coupling as represented by (2) and Table I. However if the effect of coupling between the aircraft dynamics and the wind gradient can be neglected, the effect of wind on the control boundaries is not dependent on the shape of the wind profile, but on the integration of that profile. Therefore an averaged value for the wind effect can be determined from a (forecast) wind profile on descent by

$$w_{crs} = 2\frac{\int_{H_p=0}^{H_{p_{crs}}} w(H_p)\,dH_p}{H_{p\,crs}}, \qquad (4)$$

where the factor '2' accounts for the model-assumed linear varying wind from null wind on the ground to w_{crs} at cruise conditions.

Regression techniques were applied to find a continuous relationship describing these control boundaries, a third order fit was found to provide sufficient accuracy,

$$\begin{aligned} V_{\mathrm{CAS}_{\pm 60s@OF}} = {} & d_0 + d_1 H_{p_{crs}} + d_2 w_{crs} + d_3 M + d_4 H_{p_{crs}}{}^2 \\ & + d_5 w_{crs}{}^2 + d_6 M^2 + d_7 H_{p_{crs}} w_{crs} + d_8 H_{p_{crs}} M \\ & + d_9 w_{crs} M + d_{10} H_p{}^3 + d_{11} w_{crs}{}^3 + d_{12} M^3 \\ & + d_{13} H_{p_{crs}} w_{crs} M + d_{14} H_{p_{crs}} w_{crs}{}^2 + d_{15} H_{p_{crs}} M^2 \\ & + d_{16} H_{p_{crs}} w_{crs} + d_{17} H_{p_{crs}}{}^2 M + d_{18} w_{crs} M^2 \\ & + d_{19} w_{crs}{}^2 M \end{aligned}, \qquad (5)$$

where $H_{p_{crs}}$ is the initial cruising altitude and w_{crs} the headwind/tailwind at cruise conditions. The coefficients d_i for the B738 are given in Table II.

Fig. 9 is similar to Fig. 7 but now the control margins for 60 seconds adjustment at the Outer Fix are introduced (dotted white lines). The area of applicability of the optimal Mach/CAS coupling has reduced. Upon reaching the control boundaries, speed control can still be applied to absorb more delay (or further speed up), but the approximate-optimal relation can no longer be followed. Instead, at the intersection, the control boundary needs to be followed to provide optimal time adjustment within the applied constraints (Fig. 10). Theoretically, the control boundary, or constraint, is now providing the line of lowest dFb/dT .

As mentioned previously, there is a threshold point after which it is no longer efficient to absorb delay by speed control, and instead path stretching should be applied. This threshold point is given by the Mach/CAS combination leading to the lowest fuel burn, which is the speed schedule for optimum range, or zero Cost Index. In Fig. 10 this point is illustrated by the star as the speed schedule with lowest fuel burn along the approximate-optimal relation (2). Note that the cruise Mach number in this speed schedule can be different to the economy cruise speed due to the contribution of the descent. As a rule of thumb, the following relation was empirically determined for the Mach number below which path stretching instead of further speed control should be applied as to optimally absorb further delay,

$$M_{SWITCH} = g_0 + g_1 H_p + g_2 H_p{}^2 . \quad (6)$$

The coefficients for the B738 are provided in Table III. Obviously, the ability to path stretch might be limited due to operational constraints and other traffic, and in such a case the further speed control should be applied.

When an aircraft is required to speed up, there is little more time that can be gained by following the upper boundary as illustrated by Fig. 10. Practically, this means that when the upper boundary is reached, an aircraft can still

TABLE III
COEFFICIENTS FOR PATH STRETCH SWITCH (B738)

		Coefficients
g_0	[-]	-3.38E-01
g_1	[ft^{-1}]	5.42E-05
g_2	[ft^{-2}]	-6.60E-10

be sped up, and if done so, there might not be enough flexibility left to speed the aircraft further up in a later stage of the flight to correct for estimated arrival time drift. In such a case the aircraft might not be able to meet the original STA at the runway threshold and requires being re-sequenced. This creates instabilities in the sequence as also other aircraft require being re-sequenced.

In the appendix of this paper the solution space based on the derived relations is provided for a number of cruising altitudes. Similar to before, the headwind (HW) and tailwind (TW) cases have been modelled based on a linear changing wind from null wind on the ground to 100kts wind at FL410. In addition a null wind (NW) case has been modelled.

With all relations determined, the algorithms to find sequence resolutions in terms of the proposed concept can be finalised. As proposed by the concept a first sequence resolution will be provided near the proposed arrival manager horizon of 250NM. Fig. 11 provides an overview of the algorithm in terms of the relations previously derived in this paper. In essence finding the sequence resolution is performed by iterating a single variable, the cruise Mach number, with which the other variable, descent CAS, is related such that the fuel burn is minimised within the given constraints. These constraints are related to allowing sufficient control margin to adjust the trajectory once again closer to destination as of natural drift in the ETA. The parameters M_{LWR} and M_{UPR} are the Mach numbers at which the optimal relation (2) intersects the lower and upper boundary relations (4) respectively,

$$M_{LWR} = M: \quad V_{\mathrm{CAS}_{\mathrm{OPT}}}(M) = V_{\mathrm{CAS}_{-60s@OF}}(M), \quad (7)$$

$$M_{UPR} = M: \quad V_{\mathrm{CAS}_{\mathrm{OPT}}}(M) = V_{\mathrm{CAS}_{+60s@OF}}(M). \quad (8)$$

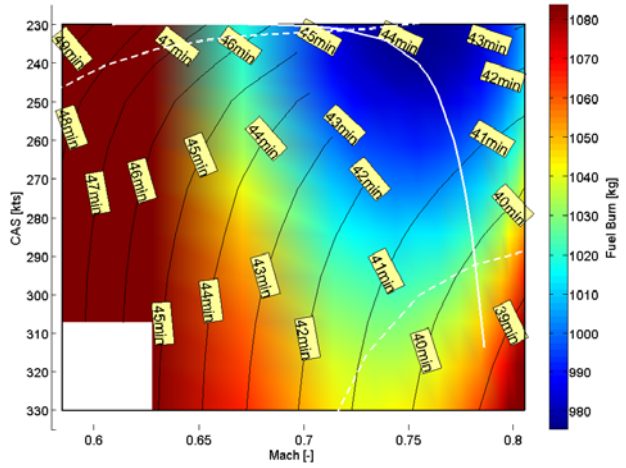

Figure 9: Solution space for B738/250NM/FL350 with control boundaries.

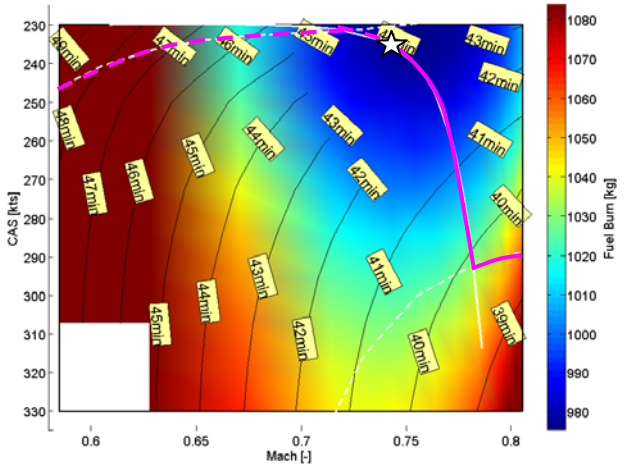

Figure 10: Optimal solutions for B738/250NM/FL350 with constraints.

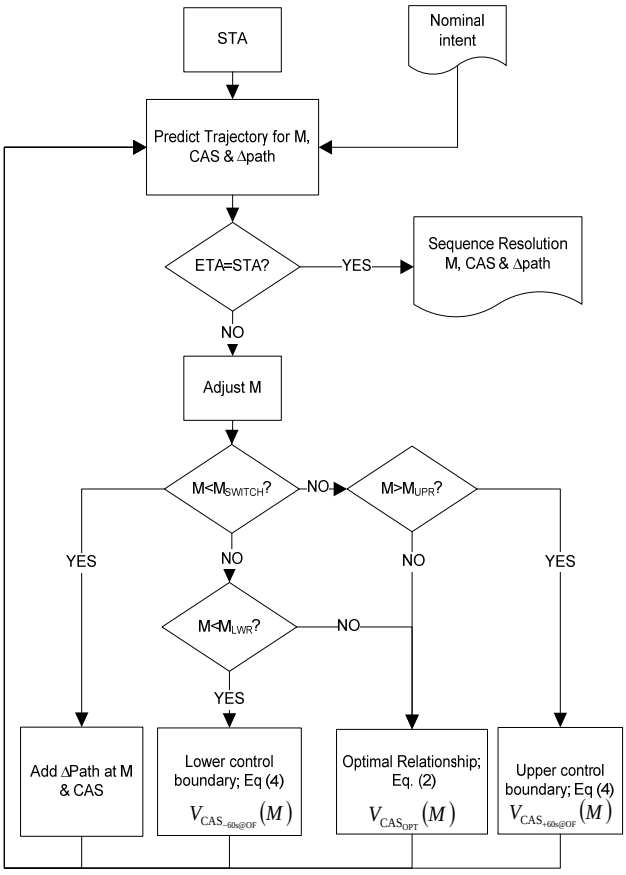

Figure 11: Algorithm for sequence resolution at 250NM horizon.

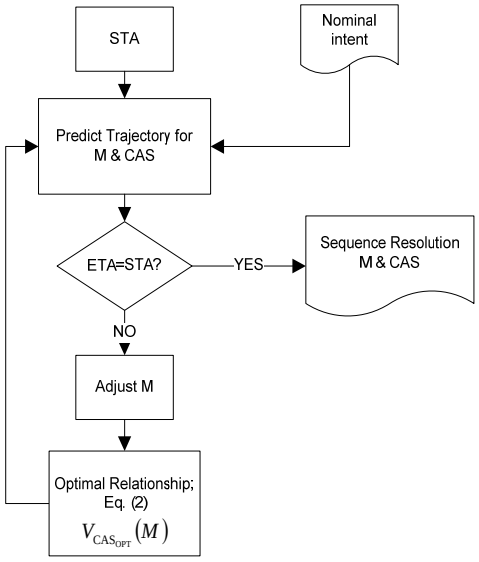

Figure 12: Algorithm for sequence resolution at Outer Fix.

A second sequence resolution occurs at the Outer Fix to account for drift in the ETA or other unforeseen changes. By use of the algorithm in Fig. 11, sufficient control in terms of descent speed adjustment should be available such that no adjustment to the lateral path is required. As discussed previously, adjustment of the lateral path after TOD should be avoided to maintain the integrity of a structured TMA. The sequence resolution provided at the Outer Fix therefore simply follows the optimal relation (2); the algorithm is presented in Fig. 12.

With the revised descent speed it is envisioned that the scheduled time at the Metering Fix at TMA entry is met within 30 seconds tolerance. Precise sequencing to closely meet the scheduled time at the threshold can be performed by small TMA speed adjustments or radar vectoring in the circuit area (if possible and at minimum), however not detailed in this paper.

The previous derived relations and coefficients are dependent on aircraft type. This paper used the B738 to illustrate the methodology, but it can easily be extended to include different aircraft types, or aircraft families. In the appendix of this paper coefficients are provided for the Boeing 777-300 (B773) and Boeing 767-300 (B763) to illustrate this.

Note that the presented methodology focuses on the relationship between the different degrees of freedom available to provide sequence resolutions, e.g. cruise Mach, descent CAS, and path stretch. The simulated simplified operations were only used to derive these relationships; the associated calculated flight times are therefore just an indication and should not directly be used by the DST. Instead, the DST is envisioned to apply an iterative process using a high fidelity trajectory predictor and the derived relationships to find the required trajectory adjustment to match an aircraft's predicted arrival time with the scheduled arrival time (Fig. 6).

IV. Conclusion

This paper presented a methodology and algorithm to provide speed advisories to meet a certain scheduled arrival time at the destination. The methodology provides a generic algorithm and relations that allow for the iteration in a single variable, cruise Mach number, to find a speed schedule meeting the scheduled arrival time, while minimising fuel burn and allowing sufficient control margin. This control margin is required to allow for possible later adjustments to account for time drift. In combination with a proposed multi-stage arrival metering concept, this methodology enables aircraft to be sequenced for arrival by instructing a descent speed schedule and allowing them to perform a continuous descent without relying on airborne capabilities to actively control to an arrival time.

The presented methodology provides sequence resolutions for individual aircraft. These resolutions will need to be considered in the context of a multitude of aircraft to provide separation assurance and can possibly be integrated with automated conflict detection tools.

APPENDIX

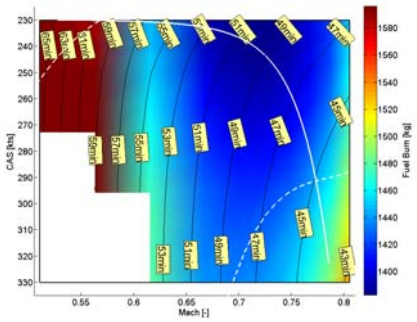

Figure 13: Solution space B738/250NM/FL300 (HW).

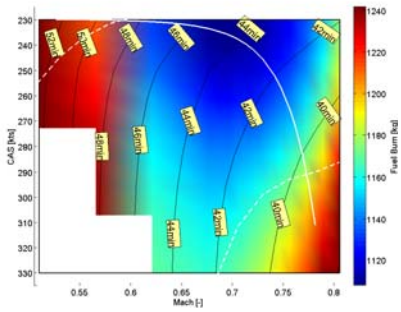

Figure 14: Solution space B738/250NM/FL300 (NW).

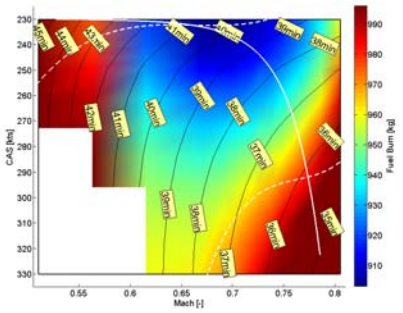

Figure 15: Solution space B738/250NM/FL300 (TW).

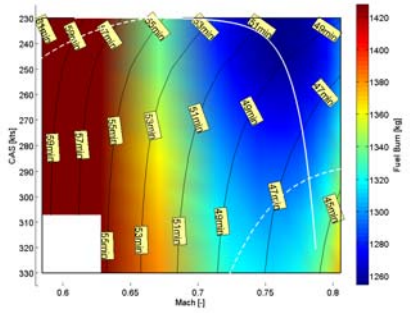

Figure 16: Solution space B738/250NM/FL350 (HW).

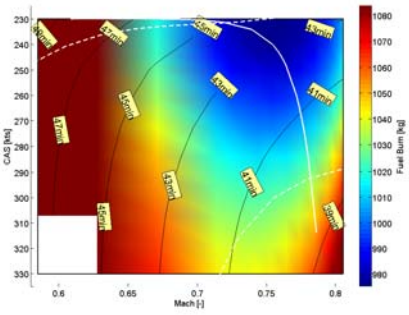

Figure 17: Solution space B738/250NM/FL350 (NW).

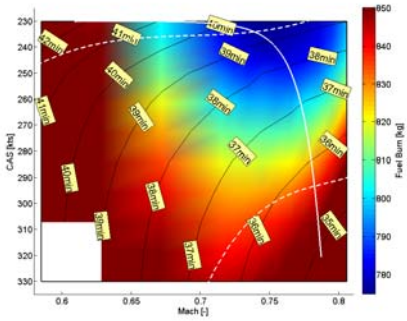

Figure 18: Solution space B738/250NM/FL350 (TW).

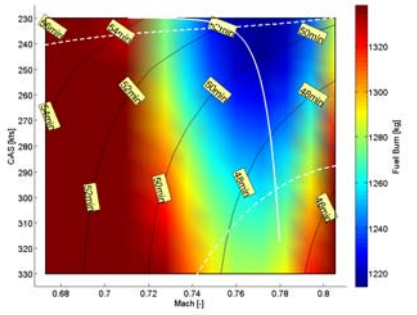

Figure 19: Solution space B738/250NM/FL400 (HW).

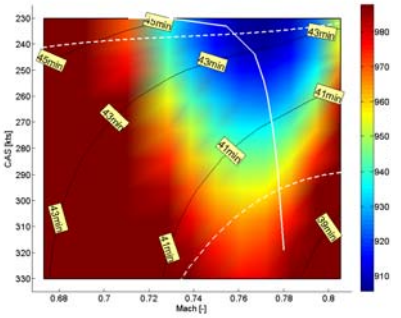

Figure 20: Solution space B738/250NM/FL400 (NW).

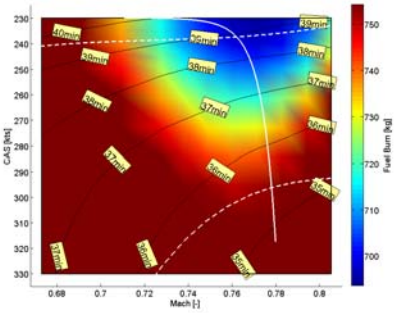

Figure 21: Solution space B738/250NM/FL400 (TW).

TABLE VI
COEFFICIENTS FOR B763

Altitude	Coefficients for Optimal Mach/CAS Relationship				
	c_1 [kts]	c_2 [-]	c_3 [-]	$V_{CASoffset}$ [kts]	M_{offset} [-]
FL270	3.16E-01	1.52E+01	8.46E+00	229.5	0.478
FL280	3.51E-01	1.16E+01	2.09E+01	229.5	0.493
FL290	4.54E-01	-5.28E-01	5.98E+01	229.5	0.501
FL300	5.01E-01	-4.27E+00	7.72E+01	229.5	0.518
FL310	6.33E-01	-1.33E+01	1.10E+02	229.5	0.527
FL320	6.64E-01	-1.63E+01	1.33E+02	229.5	0.547
FL330	6.49E-01	-1.60E+01	1.40E+02	229.5	0.558
FL340	6.17E-01	-1.49E+01	1.46E+02	229.5	0.570
FL350	5.32E-01	-9.85E+00	1.39E+02	229.5	0.582
FL360	4.75E-01	-5.47E+00	1.37E+02	229.5	0.595
FL370	4.56E-01	-3.34E+00	1.43E+02	229.5	0.607
FL380	3.76E-01	6.83E+00	1.35E+02	229.5	0.634
FL390	3.08E-01	1.70E+01	1.11E+02	229.5	0.648
FL400	2.81E-01	2.97E+01	6.88E+01	229.5	0.664
FL410	2.05E-01	5.11E+01	-2.67E+01	229.5	0.682

Coefficient for Path Stretch Switch	
g_0	-1.16E+00
g_1	1.02E-04
g_2	-1.32E-09

Coefficients for Control Boundaries			
		High speed boundary (+60 s)	Low speed boundary (-60 s)
d_0	[kts]	1.14E+04	8.13E+02
d_1	[kts/ft]	2.47E-01	2.58E-02
d_2	[-]	-7.18E+00	-6.84E-02
d_3	[kts]	-5.01E+04	-3.90E+03
d_4	[kts/ft^2]	8.62E-07	1.11E-07
d_5	[kts^{-1}]	-9.77E-03	-3.83E-04
d_6	[kts]	7.36E+04	7.36E+03
d_7	[ft^{-1}]	-4.29E-04	-5.05E-05
d_8	[ft^{-1}]	-6.55E-01	-7.65E-02
d_9	[-]	3.43E+01	3.17E+00
d_{10}	[kts/ft^3]	0	0
d_{11}	[kts^{-2}]	2.58E-04	-5.40E-05
d_{12}	[kts]	-3.54E+04	-4.02E+03
d_{13}	[ft^{-1}]	3.89E-04	1.06E-04
d_{14}	[ft^{-1} kts^{-1}]	-6.01E-08	-1.59E-09
d_{15}	[kts/ft]	7.71E-01	1.42E-01
d_{16}	[ft^{-1}]	0	0
d_{17}	[kts/ft^2]	-9.90E-07	-4.46E-08
d_{18}	[-]	-2.84E+01	-5.20E+00
d_{19}	[kts^{-1}]	1.36E-02	5.98E-04

TABLE VII
COEFFICIENTS FOR B773

Altitude	Coefficients for Optimal Mach/CAS Relationship				
	c_1 [kts]	c_2 [-]	c_3 [-]	$V_{CAS_{offset}}$ [kts]	M_{offset} [-]
FL270	2.74E-01	2.04E+01	-3.89E+00	229.5	0.526
FL280	3.56E-01	1.05E+01	4.11E+01	229.5	0.546
FL290	4.23E-01	1.83E+00	7.73E+01	229.5	0.557
FL300	3.92E-01	5.51E+00	7.29E+01	229.5	0.580
FL310	4.85E-01	-5.37E+00	1.26E+02	229.5	0.595
FL320	4.65E-01	-2.74E+00	1.24E+02	229.5	0.610
FL330	4.87E-01	-6.37E+00	1.57E+02	229.5	0.626
FL340	4.40E-01	-1.52E+00	1.84E+02	229.5	0.658
FL350	3.74E-01	1.32E+01	1.36E+02	229.5	0.677
FL360	3.68E-01	1.30E+01	1.48E+02	229.5	0.683
FL370	3.31E-01	2.26E+01	1.43E+02	229.5	0.703
FL380	3.40E-01	4.41E+01	4.29E+01	229.5	0.725
FL390	3.28E-01	4.52E+01	4.39E+01	229.5	0.727
FL400	3.29E-01	3.73E+01	1.16E+02	229.5	0.727
FL410	4.33E-01	1.31E+02	-7.15E+02	229.5	0.778

Coefficient for Path Stretch Switch	
g_0	-7.96E-02
g_1	4.66E-05
g_2	-6.04E-10

Coefficients for Control Boundaries			
		High speed boundary (+60 s)	Low speed boundary (-60 s)
d_0	[kts]	1.82E+03	5.36E+02
d_1	[kts/ft]	1.56E-01	1.99E-02
d_2	[-]	-1.24E+00	2.76E-01
d_3	[kts]	-1.20E+04	-2.18E+03
d_4	[kts/ft^2]	8.21E-07	1.79E-07
d_5	[kts^{-1}]	-1.15E-03	-8.88E-06
d_6	[kts]	2.29E+04	4.36E+03
d_7	[ft^{-1}]	-8.05E-05	-1.86E-05
d_8	[ft^{-1}]	-4.23E-01	-6.50E-02
d_9	[-]	6.01E+00	3.15E-01
d_{10}	[kts/ft^3]	0	0
d_{11}	[kts^{-2}]	0	0
d_{12}	[kts]	-1.30E+04	-2.63E+03
d_{13}	[ft^{-1}]	9.91E-05	2.02E-05
d_{14}	[ft^{-1} kts^{-1}]	3.07E-08	-3.14E-09
d_{15}	[kts/ft]	7.71E-01	1.42E-01
d_{16}	[ft^{-1}]	0	0
d_{17}	[kts/ft^2]	-9.90E-07	-1.05E-06
d_{18}	[-]	-2.84E+01	-5.55E+00
d_{19}	[kts^{-1}]	1.36E-02	-6.96E-05

REFERENCES

[1] Joint Planning and Development Office. (2007). *Concept of Operations for the Next Generation Air Transportation System*. Washington: Joint Planning and Development Office.

[2] SESAR Consortium. (2007). *The ATM Target Concept (D3)*.

[3] SESAR JU. (2012). *i4D+CTA Validation Report - Step A*.

[4] CASSIS Project Partners. (2010). *CTA/ATC System Integration Studies 2 (CASSIS) Flight Trials Report*.

[5] McDonald, G.N., & Bronsvoort, J. (2012). *Concept of Operations for ATM by Managing Uncertainty through Multiple Metering Points.* Proceedings of the Air Transport and Operations Symposium, Delft, The Netherlands.

[6] Erzberger, H., & Chapel, J.D. (1984). *Concepts and Algorithms for Terminal-Area Traffic Management*. Moffet Field, CA: NASA Ames Research Center.

[7] Erzberger, H., & Tobias, L. (1986). *A Time-Based Concept for Terminal-Area Traffic Management*. Washington, DC: National Aeronautics and Space Administration.

[8] Coppenbarger, R.A., Lanier, R., Sweet, D.N., & Dorsky, S. (2004). *Design and Development of the En Route Descent Advisor (EDA) for Conflict-Free Arrival Metering.* Proceedings of the AIAA Guidance, Navigation, and Control Conference and Exhibit, Providence, RI.

[9] Coppenbarger, R.A., Mead, R.W., & Sweet, D.N. (2007). *Field Evaluation of the Tailored Arrivals Concept for Datalink-Enabled Continuous Descent Approach.* Proceedings of the 7th AIAA Aviation Technology, Integration and Operations Conference (ATIO), Belfast, Northern Ireland.

[10] Kok, B.B., & Bailey, L. (2007). *Speed And Route Advisor (SARA) Project plan P1557* (Project Plan No. KDC-2007-0040 version 0.6). Amsterdam: LVNL, Air Traffic Control the Netherlands, Boeing, Eurocontrol MUAC.

[11] Dijkstra, F., Mijatovic, D., & Mead, R. (2011). Design Options for Advanced Arrival Management in the SESAR Context. *Air Traffic Control Quarterly, Vol 19(1)*, 23-39.

[12] Bronsvoort, J., McDonald, G.N., Porteous, R.K., & Gutt, E. (2009). *Study of Aircraft Derived Temporal Prediction Accuracy using FANS.* Proceedings of the 13th Air Transport Research Society, Abu Dhabi.

[13] Raynaud, S. (2011). *ETA Uncertainty - Technical Report* (White paper). Toulouse: Airbus.

[14] De Smedt, D. & Robert, E. (2011). *WG-85 Navigation "Initial 4D" White Paper - ETA uncertainty in closed loop* (No. WG85-03).

[15] Airbus. (1998). *Getting to Grips with Cost Index* (Customer service brochure): Airbus Industrie.

[16] Airbus. (2004). *Getting to Grips with Fuel Economy*: Airbus Industries.

[17] Jackson, M.R.C., & O'Laughlin, B.E. (2007). *Airborne Required Time of Arrival Control and Integration with ATM.* Proceedings of the 7th AIAA Aviation Technology, Integration and Operations Conference (ATIO), Belfast, Northern Ireland.

[18] López Leonés, J., Vilaplana, M.A., Gallo, E., Navarro, F.A., & Querejeta, C. (2007). *The Aircraft Intent Description Language: A key enabler for Air-Ground synchronization in Trajectory-Based Operations.* Proceedings of the 26th Digital Avionics Systems Conference, Dallas, TX, USA.